Electron-phonon interaction and ultrasonic attenuation in the ruthenate and cuprate superconductors

M. B. Walker, M. F. Smith, and K. V. Samokhin
Department of Physics, University of Toronto, Toronto, Ontario, Canada M5S 1A7
(Received 7 May 2001; revised manuscript received 17 July 2001; published 11 December 2001)

This article derives an electron-phonon interaction suitable for interpreting ultrasonic attenuation measurements in the ruthenate and cuprate superconductors. The huge anisotropy found experimentally [C. Lupien *et al.*, Phys. Rev. Lett. **86**, 5986 (2001)] in Sr_2RuO_4 in the normal state is accounted for in terms of the layered square-lattice structure of Sr_2RuO_4, and the dominant contribution to the attenuation in Sr_2RuO_4 is found to be due to electrons in the γ band. The experimental data in the superconducting state are found to be inconsistent with vertical line nodes in the gap in either the (100) or (110) plane. Also, a general method, based on the use of symmetry, is developed to allow for analysis of ultrasonic attenuation experiments in superconductors in which the electronic band structure is complicated or not known. Our results, both for the normal-state anisotropy and relating to the positions of the gap nodes in the superconducting state, are different from those obtained from analyses using a more traditional model for the electron-phonon interaction in terms of an isotropic electron stress tensor. Also, a brief discussion of the ultrasonic attenuation in UPt_3 is given.

DOI: 10.1103/PhysRevB.65.014517 PACS number(s): 74.25.Ld, 74.20.Rp

I. INTRODUCTION

This article describes a theory of ultrasonic attenuation in the ruthenate and cuprate superconductors. It has been stimulated largely by the work of Lupien *et al.*[1] which presented the results of detailed experimental measurements of ultrasonic attenuation in both the normal and superconducting states of Sr_2RuO_4. The goal of that work was to use ultrasonic attenuation as a tool to gain information on the presence and location of nodes in the superconducting gap. Quite unexpectedly, however, they found a huge anisotropy in the measured attenuation, even in the normal state. Some of their results are shown in Fig. 1. Notice that the normal-state attenuation of the longitudinal wave propagating along the [110] direction is lower by a factor of approximately 30 than that of the [100] longitudinal wave. Furthermore, the attenuation of the transverse wave along the [100] direction is lower than that of the transverse wave along the [110] direction by a factor of more than 1000. Lupien *et al.* note that their results indicate the need for a new theory of the electron-phonon interaction allowing for a significant variation of the different sound-wave modes. They also suggest that the lack of a reliable theory of ultrasonic attenuation in Sr_2RuO_4 has greatly hindered the use of this technique as a tool for gaining information about the location of the gap nodes in this material.

The use of ultrasonic attenuation as a tool to locate the positions of nodes in the energy gaps of superconductors has been described, for example, by Moreno and Coleman.[2] In their model, the phonon strain field couples to a stress tensor describing the flow of electron momentum. The electron stress tensor is taken to be that appropriate to an isotropic electron fluid. This approach, which can be traced back to early work on ultrasonic attenuation in heavy-fermion superconductors,[3–5] in *s*-wave superconductors,[7,8] and in normal metals,[9] has also been used in the most recent attempts to understand ultrasonic attenuation in Sr_2RuO_4.[10,11] The use of an electron stress tensor appropriate to an isotropic fluid gives an elegant and simple formulation of the theory. However, it seems clear that a new approach is needed if one wishes to be able to account in detail for the ultrasonic attenuation observed in the recent experiments on Sr_2RuO_4. The approach developed in this article takes account of the crystalline and electronic structure of Sr_2RuO_4, but also can be shown to reduce to the traditional isotropic electron–stress-tensor approach in an appropriate limit (this limit not being appropriate for Sr_2RuO_4).

This article shows that the strong anisotropy of the ultrasonic attenuation in Sr_2RuO_4 is intimately connected with its layered square-lattice structure. We start from the idea that the electronic structure of Sr_2RuO_4 in the neighborhood of the Fermi surface can be well described in terms of a simple tight-binding Hamiltonian,[12,13] in which a central role is played by hopping matrix elements describing the hopping of an electron from one ruthenium ion to a nearest-neighbor or next-nearest-neighbor ruthenium ion. To develop a model for the electron-phonon interaction, we assume that the hopping matrix element depends on the distance between the ions, so that if a sound wave stretches the distance between two ions, the matrix element describing the hopping of an electron between these two ions changes. It is easily seen that a transversely polarized sound wave traveling in the [100] direction in the ruthenium-ion square lattice does not stretch the nearest-neighbor bond between two ruthenium ions and, hence, is not coupled to the electrons (at least by a nearest-neighbor coupling). This is the reason for the extremely low attenuation of the T100 sound wave reported in Ref. 1 (see Fig. 1). It is also easily seen that for a two- or three-dimensional hexagonal lattice or for a three-dimensional body-centered or face-centered lattice, or if the next-nearest-neighbor interaction is large, this argument does not apply. Thus the highly unusual strongly anisotropic ultrasonic attenuation observed in Sr_2RuO_4 is directly related to the layered square-lattice structure of this material. The an-

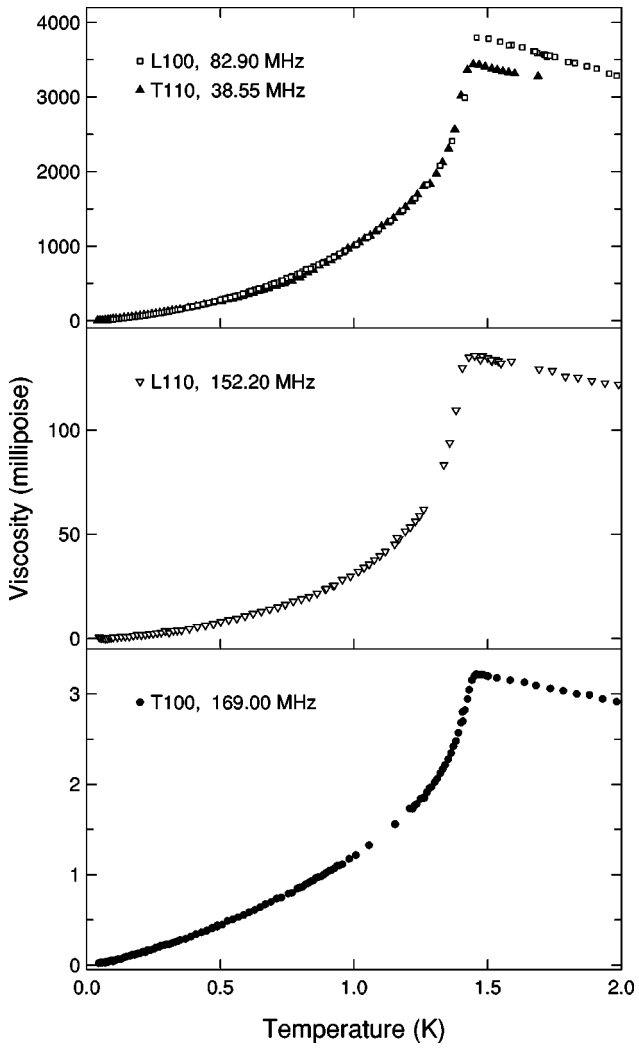

FIG. 1. Experimental data on the mode viscosity for the four in-plane sound-wave modes taken from Ref. 1. The mode viscosity η plotted here is related to the attenuation α by the formula $\eta = \alpha\rho v_s^3/(2\pi\nu)^2$, where ρ is the density, v_s is the sound velocity, and ν is the frequency. All sound-wave modes have both the direction of propagation and the polarization lying in the basal plane. The nature of the mode (L for longitudinal and T for transverse) as well as the Miller indices of the propagation direction are shown in the figure.

isotropy in the attenuation of longitudinal waves (e.g., for the L100 and L110 waves of Fig. 1) also finds an elementary qualitative and quantitative explanation in terms of the model developed in detail below: this explanation depends on the details of the Fermi surface geometry and will be given later.

After developing a detailed model for the electron-phonon interaction in Sr_2RuO_4 and confirming that the model accounts well for the ultrasonic attenuation in the normal state, we proceed to an analysis of the ultrasonic attenuation in the superconducting state with the objective of gaining information on the positions of nodes in the superconducting energy gap. The basic ideas here have been clearly set out in the article by Moreno and Coleman.[2] They show that for a given sound-wave propagation direction and polarization, the nodes in the gaps can be described as either ''active'' or ''inactive'' and that the temperature dependence of the ultrasonic attenuation is very different in the two cases. These ideas are described in greater detail below and exploited to gain information on the positions of the gap nodes in Sr_2RuO_4. Our calculations are done in the hydrodynamic limit. The opposite (''quantum'') limit relevant for either very pure samples, or very high frequencies, has been considered in Ref. 14.

A consequence of our work is the recognition that the traditional isotropic electron–stress-tensor model of the electron-phonon interaction makes certain nodes ''accidentally'' inactive for the case of longitudinal sound waves. This accidental inactivity is a consequence of the fact that the isotropic electron–stress-tensor model of the electron-phonon interaction is not sufficiently general to describe realistically the electron-phonon interaction. In a more realistic model, all nodes are active for longitudinal phonons. Thus, the isotropic electron–stress-tensor model for the electron-phonon model gives misleading results for the temperature dependence of the ultrasonic attenuation associated with longitudinal phonon modes in some cases and should not be used in studies aimed at determining the positions of the nodes in the gap of an unconventional superconductor.

Although the emphasis in this article will be on ultrasonic attenuation in Sr_2RuO_4 because of the availability of experimental data for this material,[1] it should be noted that our detailed results for the γ band are also applicable (except for the interlayer interaction) to cuprate superconductors such as $YBa_2Cu_3O_{6+x}$; furthermore, it is a simple matter to develop an appropriate interlayer electron-phonon interaction for the $YBa_2Cu_3O_{6+x}$ structure analogous to the result for Sr_2RuO_4 developed here. The analysis in Sec. V allows us to make some general statements about the symmetry-imposed properties of the electron-phonon interaction and their manifestations for the ultrasonic attenuation in unconventional superconductors, in particular, in UPt_3.

The discovery[15] of superconductivity in the layered perovskite Sr_2RuO_4 and the proposal[16] that the superconducting Cooper pairs in that material formed in a spin-triplet state have stimulated considerable interest and study (see Ref. 17 for a review of the properties of Sr_2RuO_4, and Ref. 18 for a review of the symmetry classification and the physical properties of unconventional superconductors in general). Until recently, it was thought that the superconducting order in Sr_2RuO_4 could be described by the order parameter $\mathbf{d}(\mathbf{k}) \propto \hat{\mathbf{z}}(k_x + ik_y)$.[12,16] Because the Fermi surface of Sr_2RuO_4 has a quasi-two-dimensional cylindrical form[19] with no points at $k_x = k_y = 0$, the Fermi surface for this order parameter is fully gapped. More recently, however, power-law temperature dependences more characteristic of a gap having line nodes have been found in a number of experiments, including specific heat,[20,21] nuclear quadrupole resonance (NQR),[22] penetration depth,[23] thermal conductivity,[24,25] and ultrasonic attenuation.[1] It is not easy to reconcile the presence of triplet Cooper pairs, a broken-time-reversal symmetry, and line nodes in the gap. A number of proposals to do so have nevertheless been made. These include spin-triplet states charac-

terized by vectors $\mathbf{d}(\mathbf{k})$ of the form $\mathbf{d}(\mathbf{k}) \propto \hat{\mathbf{z}}[\sin(k_x a) + i \sin(k_y a)]$ (Refs. 26–28) and having vertical line nodes in (100) planes, so-called *f*-wave states characterized by $\mathbf{d}(\mathbf{k}) \propto \hat{\mathbf{z}}(k_x + ik_y)k_x k_y$ or by $\mathbf{d}(\mathbf{k}) \propto \hat{\mathbf{z}}(k_x + ik_y)(k_x^2 - k_y^2)$,[10,11,27,29] having vertical line nodes in (100) and (110) planes, respectively, by *f*-wave states characterized by $\mathbf{d}(\mathbf{k}) \propto \hat{\mathbf{z}} k_z (k_x + ik_y)^2$ (Refs. 2, 31, and 32) and having horizontal lines nodes in the plane $k_z = 0$, by states characterized by $\mathbf{d}(\mathbf{k}) \propto \hat{\mathbf{z}}(k_x + ik_y)\cos(k_z c)$ (Ref. 29) and having horizontal line nodes in the plane $k_z = \pi/(2c)$, or by states characterized by $\mathbf{d}(\mathbf{k}) \propto \hat{\mathbf{z}}[\sin(k_x a/2)\cos(k_y a/2) + i \cos(k_x a/2)\sin(k_y a/2)]\cos(k_z c/2)$ (Refs. 29 and 30) and having horizontal line nodes in the plane $k_z = \pi/c$. The analysis of the ultrasonic attenuation experiments given below allows many of these possibilities to be ruled out and suggests that attention be focused on those possibilities characterized by the existence of horizontal line nodes.

The structure of the article is as follows. Section II develops a tight-binding model of the electron-phonon interaction accounting for the details of the layered square-lattice structure occurring in the ruthenate and cuprate superconductors. Section III evaluates a formula giving the ultrasonic attenuation in the normal state of Sr_2RuO_4 in terms of the model electron-phonon interaction given in Sec. II and shows that the extremely strong and unusual anisotropy of the attenuation is accounted for by the model. Section IV makes use of the model electron-phonon interaction to determine the activity or inactivity of the gap nodes for various proposed superconducting gap structures for Sr_2RuO_4, thus allowing statements to be made about which of the various proposals for the gap structure are consistent with the experimental ultrasonic attenuation data. Section V shows that a detailed model of the electron-phonon interaction is not necessary to determine which nodes in the superconducting state are active or inactive by showing how to obtain such information from symmetry arguments only. Such arguments are sufficiently powerful to be applicable to cases where the development of a detailed model of the electron-phonon interaction is not available. Our detailed model for Sr_2RuO_4 is shown to be consistent with these arguments (although the isotropic electron stress tensor model is not), and furthermore, some new results relating to the interpretation of ultrasonic attenuation in UPt_3 are presented. The Appendix gives a discussion of the universality of the low-temperature, temperature-independent contribution to the attenuation in the superconducting state, showing that the presence (or absence) of universal behavior is associated with the activity (or inactivity) of the gap nodes.

II. ELECTRON-PHONON INTERACTION IN LAYERED CUPRATE AND RUTHENATE SUPERCONDUCTORS

The approximate two-dimensional nature[19] of the Fermi surface of Sr_2RuO_4 suggests that it can be described, to a first approximation, in terms of electrons interacting principally through intraplanar interactions. The Fermi surface consists of three sheets (see Fig. 2), which can be thought of as being derived from the three ruthenium orbitals d_{xy}, d_{xz}, and d_{yz}.[17,33,34] The Hamiltonian describing the band structure of a single plane can thus be written[12]

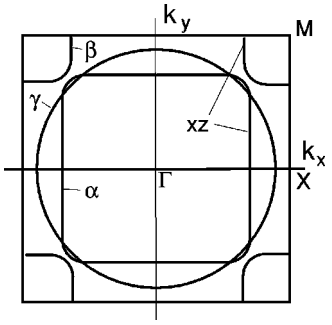

FIG. 2. Schematic of the Fermi surface of $Sr_2Ru_2O_4$ showing the α, β, and γ bands. Also shown are portions of the α and β bands that are predominantly xz in character.

$$H_{plane} = \sum_{\nu,\nu',\mathbf{n},\mathbf{n}',\sigma} t_{\nu,\nu'}(\mathbf{r}_{\mathbf{n}} - \mathbf{r}_{\mathbf{n}'}) c^{\dagger}_{\nu,\mathbf{n},\sigma} c_{\nu',\mathbf{n}',\sigma}, \qquad (1)$$

where $c^{\dagger}_{\nu,\mathbf{n},\sigma}$ creates an electron with spin σ in the νth ($\nu = \{xy, xz, yz\}$) ruthenium orbital on the ruthenium ion at the site $\mathbf{n}$ of the ruthenium square lattice. Because of the σ_z plane of reflection symmetry at the center of the RuO_4 plane, there is no overlap between the xy orbitals and those of xz and yz symmetry. This means that one sheet of the Fermi surface (the γ sheet) can be attributed to the xy orbitals, while the α and β sheets result from hybridization of the xz and yz orbitals. Also, from symmetry, there is no nearest-neighbor overlap between the xz and yz orbitals, while the largest overlap integral for an xz orbital is expected to be with nearest-neighbor ions in the $\pm x$ directions, since the lobes of these orbitals point in these directions rather than in the $\pm y$ directions. This means that the xz and yz orbitals form approximately independent one-dimensional bands, with the hybridization of these bands giving relatively small perturbations to the energies, except where the bands cross. A schematic view of the Fermi surface is shown in Fig. 2.

To derive an expression for the electron-phonon interaction, we assume that the hopping matrix elements in Eq. (1) in the vibrating lattice depend on the instantaneous positions of the ruthenium ions, $\mathbf{r}_{\mathbf{n}} = \mathbf{r}^{(0)}_{\mathbf{n}} + \mathbf{u}_{\mathbf{n}}$, where $\mathbf{r}^{(0)}_{\mathbf{n}}$ is the equilibrium position of the ion at lattice site $\mathbf{n}$, and $\mathbf{u}_{\mathbf{n}}$ is its displacement from equilibrium. The lowest-order contribution to the electron-phonon interaction is found by expanding the hopping matrix elements in powers of the ionic displacements $\mathbf{u}_{\mathbf{n}}$ and keeping only linear terms. First consider doing this for only the nearest-neighbor hopping matrix elements for the xz orbitals that lie in the $\pm x$ directions relative to each other, since this is a relatively simple effectively one-dimensional case. This results in the interaction

$$H^{xz}_{e-ph,plane} = \frac{g^{xz}}{a} \sum_{\mathbf{n},\sigma} (u_{\mathbf{n},x} - u_{\mathbf{n}+\mathbf{a},x}) \times (c^{\dagger}_{xz,\mathbf{n},\sigma} c_{xz,\mathbf{n}+\mathbf{a},\sigma} + c^{\dagger}_{xz,\mathbf{n}+\mathbf{a},\sigma} c_{xz,\mathbf{n},\sigma}). \qquad (2)$$

Here $u_{\mathbf{n},x}$ is the xth component of displacement of the **n**th ion in the plane, and $u_{\mathbf{n}+\mathbf{a},x}$ refers to the ion one Bravais-lattice vector **a** in the positive x direction from the **n**th ion. Notice that, for reasons of symmetry, this expression does not contain displacements normal to the bond axis. Thus (even though we have not assumed that the forces between the ions are central), only displacements that stretch the bond distance contribute to the electron-phonon interaction in this case. Introducing the lattice Fourier transforms of the site variables in Eq. (2) and summing this Hamiltonian over all planes in the crystal, gives

$$H^{\nu}_{e-ph}=\frac{1}{\sqrt{N}}\sum_{\mathbf{q},j,\mathbf{k},\sigma,\mathbf{G}} g^{\nu}_{\mathbf{k}+\mathbf{q}/2,\mathbf{q},j}A_{\mathbf{q},j}c^{\dagger}_{\nu,\mathbf{k}+\mathbf{q}+\mathbf{G},\sigma}c_{\nu,\mathbf{k},\sigma}, \quad (3)$$

where $\nu=xz$, **G** is a reciprocal lattice vector, $A_{\mathbf{q},j}=a^{\dagger}_{-\mathbf{q},j}+a_{\mathbf{q},j}$, $a_{\mathbf{q},j}$ destroys a phonon corresponding to wave vector **q** and polarization j, and N is the total number of ruthenium ions in the crystal. The wave vectors **q** and **k** are three-dimensional wave vectors and this Hamiltonian is for the whole crystal. Here

$$g^{\nu}_{\mathbf{k}+\mathbf{q}/2,\mathbf{q},j}=g_{\mathbf{q},j}F^{\nu}_{j}(\mathbf{k},\mathbf{q}), \quad (4)$$

with

$$g_{\mathbf{q},j}=-\sqrt{2}i\left(\frac{\hbar\omega_{\mathbf{q},j}}{Mv_j^2}\right)^{1/2}, \quad (5)$$

$$F^{\nu}_{j}(\mathbf{k},\mathbf{q})=g^{\nu}\sum_{\mathbf{R}}(\hat{\mathbf{q}}\cdot\hat{\mathbf{R}})[\hat{\mathbf{R}}\cdot\mathbf{e}_j(\mathbf{q})]\cos(\mathbf{k}\cdot\mathbf{R}), \quad (6)$$

where $\omega_{\mathbf{q},j}$ is a phonon frequency, v_j is the sound velocity for a phonon of polarization j, $\mathbf{e}_j(\mathbf{q})$ is a unit vector in the direction of the phonon polarization, M is the total mass of the ions in a primitive unit cell, and a caret (as in $\hat{\mathbf{q}}$) indicates a unit vector. Since we are interested in this article only in low-frequency phonons, the expression (6) is given to the lowest nontrivial order in the phonon wave vector **q**. The result of this section for the interaction of phonons with the xz electrons as described by Eq. (2) is given by Eqs. (3), (4), (5), and (6) with $\nu=xz$ and with the sum over **R** containing a single term with **R** equal to the Bravais lattice vector **a**.

Similarly, the interaction of phonons with the yz electrons is described by Eqs. (3), (4), (5), and (6) with $\nu=yz$ and with the sum over **R** containing a single term with **R** equal to the Bravais lattice vector **b**. Also, the coupling constant is called $g^{\alpha\beta}\equiv g^{xz}=g^{yz}$.

The nearest-neighbor interaction of phonons with the xy (γ band) electrons is described by Eqs. (3), (4), (5), and (6) with $\nu=xy$ and with the sum over **R** containing two terms with **R** equal to the Bravais lattice vectors **a** and **b**. The coupling constant is called g^{γ}.

The next-nearest-neighbor interaction of phonons with the xy (γ band) electrons is described by Eqs. (3), (4), (5), and (6) with $\nu=xy$ and with the sum over **R** containing two terms with **R** equal to the Bravais lattice vectors $\mathbf{a}+\mathbf{b}$ and $\mathbf{a}-\mathbf{b}$. The coupling constant is called g'^{γ}.

So far, we have considered only electron-phonon interactions associated with the stretching of bonds between ions lying in a single plane. It is reasonable to expect these interactions to be larger than the interplanar ones because the separation between RuO_4 planes is relatively large, although this should be confirmed by comparison with experiment. However, the intraplanar interactions that we have considered so far do not affect transverse phonon modes that have their wave vector in the basal plane and their polarization perpendicular to this plane. This is because, to first order in the displacements, such phonon modes do not stretch the bond distances and, more rigorously, because the basal plane is a plane of reflection symmetry. Hence, to account for the attenuation of these phonon modes, it is necessary to consider interplanar interactions.

In describing the interplanar interactions it is reasonable to consider first interactions involving xz and yz orbitals since these orbitals have lobes sticking out of the plane, whereas the lobes of the xy orbitals lie in the plane. The fact that the parts of the Fermi surface that are made up from the xz and yz orbitals show the largest corrugations[37] along the c-axis direction support this consideration.[30] In addition we choose to consider interactions between ruthenium ions at the corner and the body center of the unit cell (which are the nearest-neighbor interplane pairs). Unfortunately, the xz and yz orbitals are not a convenient basis for describing this interaction. For this reason, the new basis $c_{\xi z}=(c_{xz}+c_{yz})/\sqrt{2}$ and $c_{\eta z}=(-c_{xz}+c_{yz})/\sqrt{2}$ will be introduced. Clearly, the ξz orbitals will interact well with themselves along body diagonals in the directions of the vectors $\mathbf{a}+\mathbf{b}+\mathbf{c}$ and $-\mathbf{a}-\mathbf{b}+\mathbf{c}$, while the ηz orbitals will interact well with each other along the body diagonals $-\mathbf{a}+\mathbf{b}+\mathbf{c}$ and $\mathbf{a}-\mathbf{b}+\mathbf{c}$.

The nearest-neighbor body-diagonal interactions between ξz orbitals are described by Eqs. (3), (4), (5), and (6) with $\nu=\xi z$ and with the sum over **R** containing two terms with **d** equal to the Bravais lattice vectors $\frac{1}{2}(\mathbf{a}+\mathbf{b}+\mathbf{c})$ and $\frac{1}{2}(-\mathbf{a}-\mathbf{b}+\mathbf{c})$. Also, the nearest-neighbor body-diagonal interactions between ηz orbitals are described by Eqs. (3), (4), (5), and (6) with $\nu=\eta z$ and with the sum over **R** containing two terms with **R** equal to the Bravais lattice vectors $\frac{1}{2}(-\mathbf{a}+\mathbf{b}+\mathbf{c})$ and $\frac{1}{2}(\mathbf{a}-\mathbf{b}+\mathbf{c})$. The coupling constants for these two interactions satisfy $g^{\xi z}=g^{\eta z}$. Because the best simple approximation to the band structure is in terms of the xz and yz states, and not in terms of the ξz and ηz states, the electron-phonon interaction derived in the ξz and ηz representation should be transformed back to the xz and yz representation.

III. ULTRASONIC ATTENUATION IN THE NORMAL STATE OF Sr_2RuO_4

As noted in the Introduction, there is an extremely strong anisotropy of the ultrasonic attenuation in the normal state of Sr_2RuO_4. This section shows how this anisotropy can be accounted for in terms of the electron-phonon interaction just described and the known Fermi-surface geometry of Sr_2RuO_4.

The attenuation constant $\alpha_j(\mathbf{q})$ for an acoustic phonon of wave vector **q** and polarization j is given by $\alpha_j(\mathbf{q})$

$=(v_j\tau_{\mathbf{q},j})^{-1}$, where $\tau_{\mathbf{q},j}$ is the phonon lifetime. Because the formula for the ultrasonic attenuation in the superconducting state is closely related to that for the normal state, the latter more general formula for the superconducting state will be given here, and the formula for the attenuation in the normal state immediately follows. The result of evaluating the phonon lifetime in the hydrodynamic limit (the electron quasiparticle mean free path much shorter than the phonon wavelength) from the self-energy of the phonon Green's function in the superconducting state is

$$\frac{1}{\tau_{\mathbf{q},j}}=\frac{16\omega_{\mathbf{q},j}^2 N_F}{\rho v_j^2}\int_0^\infty \frac{d\epsilon}{\epsilon}\left(-\frac{\partial f}{\partial \epsilon}\right) \times\langle F_j^2(\mathbf{k},\mathbf{q})\tau_{\mathbf{k}}\ \mathrm{Re}\ \sqrt{\epsilon^2-|\Delta_{\mathbf{k}}|^2}\rangle_{FS}, \tag{7}$$

where N_F is the density of states at the Fermi level in the normal state, $f(\epsilon)$ is the Fermi distribution function, and the Fermi surface average is defined by

$$\langle F_j^2(\mathbf{k},\mathbf{q})\rangle_{FS}=\frac{\int F_j^2(\mathbf{k},\mathbf{q})dS_{\mathbf{k}}/v_{\mathbf{k}}}{\int dS_{\mathbf{k}}/v_{\mathbf{k}}}. \tag{8}$$

The integration over $dS_{\mathbf{k}}$ in this equation is over all (the γ, xz, and yz) sheets of the Fermi surface, with the electron-phonon matrix element chosen appropriately for each sheet. The expression (7) is valid for all singlet superconducting phases, as well as for unitary triplet phases, for which $|\Delta_{\mathbf{k}}|^2=|\mathbf{d}(\mathbf{k})|^2$. This formula is similar to that employed in Ref. 2, except that in our expression the electron-phonon matrix element $F_j(\mathbf{k},\mathbf{q})$ replaces the isotropic electron stress tensor of Ref. 2. Also, the formula has been generalized to be applicable to anisotropic multisheet Fermi surfaces. The quantity $\tau_{\mathbf{k}}$ is the Bogoliubov quasiparticle lifetime, and for Eq. (7) to be valid, the condition $k_BT\gg\hbar/\tau_{\mathbf{k}}$ must be satisfied (see the Appendix for a more detailed discussion).

One aspect of the above discussion that is unsatisfactory is the failure to give a full treatment of the Coulomb interaction so that charge neutrality is preserved in the distorted lattice that occurs in the presence of a longitudinal sound wave. A microscopic treatment of this question for our tight-binding multiband model is beyond the scope of this article. This question has, however, been treated in early work on ultrasonic attenuation in metals with anisotropic Fermi surfaces.[35] There it was found that charge neutrality can be simply imposed in terms of an appropriately chosen spatially varying chemical potential. This leads to the same formula for the attenuation as is obtained when the charge-neutrality correction is neglected, except that the original electron-phonon matrix element is replaced by a related effective electron-phonon matrix element. Translated into our notation, their result is that the electron-phonon matrix element $F_j(\mathbf{k},\mathbf{q})$ in Eq. (7) should be replaced by the effective electron-phonon matrix element

$$\tilde{F}_j(\mathbf{k},\mathbf{q})=F_j(\mathbf{k},\mathbf{q})-\langle F_j(\mathbf{k},\mathbf{q})\rangle_{FS}. \tag{9}$$

Therefore, in what follows, Eq. (7) with F_j replaced by $\tilde{F}_j$ will be assumed to be the correct expression for the phonon relaxation rate. It should be noted that, for phonons propagating along high-symmetry directions, $\tilde{F}_j(\mathbf{k},\mathbf{q})$ differs from $F_j(\mathbf{k},\mathbf{q})$ only for longitudinal phonons.

The phonon lifetime in the normal state can be calculated from Eq. (7) by putting the superconducting energy gap equal to zero, which gives

$$\frac{1}{\tau_{\mathbf{q},j}}=\frac{8\omega_{\mathbf{q},j}^2\tau_n}{\rho v_j^2}N_F[\langle F_j^2(\mathbf{k},\mathbf{q})\rangle_{FS}-\langle F_j(\mathbf{k},\mathbf{q})\rangle_{FS}^2], \tag{10}$$

where τ_n is the electron lifetime in the normal state.

In some early work[7,9] on ultrasonic attenuation the model Hamiltonian was formulated in terms of the potential energy $V(\mathbf{x})$, assumed to be a function of the continuous electron position coordinate $\mathbf{x}$ and describing the interaction of the electron with the lattice and with impurities. In this formulation, two problems arise that are eliminated by a canonical transformation to a coordinate system fixed to the moving lattice. The first is that the perturbation of the potential due to the distorted lattice is not necessarily small. This problem does not occur in the tight-binding formulation because the perturbation is naturally formulated in terms of a strain coordinate (i.e., the ratio of the displacement to the phonon wavelength) rather than simply a displacement coordinate [see Eq. (2)]. The second problem is that it is simpler to work in a coordinate system in which the impurities are static in the zero-order Hamiltonian so that the electron's energy is conserved in the impurity scattering process. In the tight-binding approach of this article the impurities are static in the zero-order Hamiltonian. For example, potential scattering by impurities can be modeled by adding an extra term $U_{\nu,\mathbf{n}_i}c^\dagger_{\nu,\mathbf{n}_i,\sigma}c_{\nu,\mathbf{n}_i,\sigma}$ to the Hamiltonian for the νth orbital on the impurity site labeled by $\mathbf{n}_i$. There is no dependence of this impurity potential on the ion displacements, and the impurities are thus static in this representation. Thus, our approach has features qualitatively similar to those of some previous approaches,[7,9] even though the details of implementation are different.

Before proceeding further, we show that our formulation reduces to the traditional isotropic electron–stress-tensor formulation in an appropriate limit. It is known[36] that for hexagonal crystals, sound-wave propagation is isotropic with respect to rotations about the c axis. (This is not true for tetragonal crystals, such as Sr_2RuO_4.) Therefore, we expect that the isotropic electron–stress-tensor model could give an appropriate description of sound-wave attenuation in a two-dimensional hexagonal lattice, particularly if the Fermi surface is taken to be a small circle about the point $\mathbf{k}=0$ so that the electron energy spectrum can be approximated by that for free electrons, but with an effective mass. For these reasons, we consider for the moment a two-dimensional hexagonal lattice. The quantity $F_j(\mathbf{k},\mathbf{q})$ defined in Eq. (6) can be written in the form

$$F_j(\mathbf{k},\mathbf{q})=g\sum_{\alpha\beta}\hat{q}_\alpha f_{\alpha\beta}(\mathbf{k})e_{j\beta}, \tag{11}$$

where α and β are summed over the x and y components of two-dimensional vectors. Here

$$f_{\alpha\beta}(\mathbf{k}) = \sum_{\mathbf{R}} \hat{R}_\alpha \hat{R}_\beta \cos(\mathbf{k}\cdot\mathbf{R}) \tag{12}$$

and the sum over $\mathbf{R}$ is over three nearest-neighbor hexagonal Bravais-lattice vectors that make angles of 120° with each other. Now, for a Fermi surface that is a small circle surrounding the point $\mathbf{k}=0$, the approximation $\cos(\mathbf{k}\cdot\mathbf{R}) \approx 1 - \frac{1}{2}(\mathbf{k}\cdot\mathbf{R})^2$ is valid. This leads to the result

$$\begin{aligned} \tilde{f}_{\alpha\beta}(\mathbf{k}) &\equiv f_{\alpha\beta}(\mathbf{k}) - \langle f_{\alpha\beta}(\mathbf{k})\rangle_{FS} \\ &= -\tfrac{3}{8}a^2(k_\alpha k_\beta - \tfrac{1}{2}k^2\delta_{\alpha\beta}) \end{aligned} \tag{13}$$

where a is the lattice constant. This is precisely the form taken by the effective electron-phonon interaction in the isotropic electron–stress-tensor model used by many authors[2–11] and shows that our formulation of the theory of ultrasonic attenuation is equivalent to theirs in an appropriate limit.

To prepare for a more detailed study of the ultrasonic attention as observed in Ref. 1 explicit expressions for $F_j(\mathbf{k},\mathbf{q})$ [derived from Eq. (6)] are now given for our Sr_2RuO_4 model for the case that both the phonon wave vector $\mathbf{q}$ and its polarization vector $\mathbf{e}_j(\mathbf{q})$ are in the basal plane. Furthermore, a simple model of isotropic phonons is assumed in which the polarization vector is parallel to the wave vector for longitudinal phonons and perpendicular to the wave vector for transverse phonons, even when the wave vector is not along a high-symmetry direction. The direction of the phonon wave vector $\mathbf{q}$ in the basal plane is characterized by the angle ϕ that it makes with the x (i.e., a) axis.

For longitudinal phonons interacting with electrons in the γ sheet of the Fermi surface via nearest-neighbor interactions

$$F_L^\gamma(\mathbf{k},\mathbf{q}) = g^\gamma[\cos^2\phi\cos(k_x a) + \sin^2\phi\cos(k_y a)]. \tag{14}$$

For transverse T_1 phonons (T_1 phonons have their polarization as well as their wave vector in the basal plane) interacting with electrons in the γ sheet of the Fermi surface via nearest-neighbor interactions

$$F_{T1}^\gamma(\mathbf{k},\mathbf{q}) = g^\gamma\cos\phi\sin\phi[\cos(k_x a) - \cos(k_y a)]. \tag{15}$$

For longitudinal phonons interacting with electrons in the xz sheets of the Fermi surface via nearest-neighbor interactions

$$F_L^{xz}(\mathbf{k},\mathbf{q}) = g^{\alpha\beta}\cos^2\phi\cos(k_F^{\alpha\beta}a), \tag{16}$$

while for interactions with electrons in the yz sheets of the Fermi surface

$$F_L^{yz}(\mathbf{k},\mathbf{q}) = g^{\alpha\beta}\sin^2\phi\cos(k_F^{\alpha\beta}a). \tag{17}$$

In arriving at this result, this hybridization of the xz and yz bands has been neglected, as have interband transitions. The bands are thus one dimensional and characterized by the Fermi wave vector $k_F^{\alpha\beta}$.

For transverse T_1 phonons interacting with electrons in the xz sheets of the Fermi surface via nearest-neighbor interactions

$$F_{T1}^{xz}(\mathbf{k},\mathbf{q}) = -g^{\alpha\beta}\cos\phi\sin\phi\cos(k_F^{\alpha\beta}a), \tag{18}$$

while for interactions with electrons in the yz sheets of the Fermi surface

$$F_{T1}^{yz}(\mathbf{k},\mathbf{q}) = g^{\alpha\beta}\cos\phi\sin\phi\cos(k_F^{\alpha\beta}a). \tag{19}$$

Now assume that the attenuation of longitudinal phonons is dominated by their interaction with electrons on the α and β sheets of the Fermi surface as described by Eqs. (16) and (17) (and that the interaction with electrons of the γ sheet can be neglected). The attenuation will therefore be proportional to

$$\begin{aligned} \langle F_L^2\rangle_{FS} - \langle F_L\rangle_{FS}^2 &= p^{\alpha\beta}[g^{\alpha\beta}\cos(k_F^{\alpha\beta})]^2 \\ &\times(\cos^4\phi + \sin^4\phi - p^{\alpha\beta}). \end{aligned} \tag{20}$$

Here $p^{\alpha\beta}$ is defined to be the fraction of the density of states associated with the xz (or the yz) band. (The fraction of the density of states associated with the γ band is called p^γ, so that $p^\gamma + 2p^{\alpha\beta} = 1$.)

It is convenient to define the longitudinal anisotropy to be η_{l100}/η_{110} where the mode viscosities of the L100 and L110 phonons, η_{L100} and η_{L110}, respectively, are defined in the caption to Fig. 1. The experimental value of the longitudinal anisotropy is approximately 30 (see Fig. 1). The theoretical formula for the longitudinal anisotropy in the case that the attenuation is dominated by phonon interactions with electrons in the xz and yz bands is [from Eq. (20)]

$$\frac{\eta_{L100}}{\eta_{L110}} = \frac{1-p^{\alpha\beta}}{\frac{1}{2}-p^{\alpha\beta}}. \tag{21}$$

Using the experimentally determined value[19] $p^{\alpha\beta}=0.21$ gives a longitudinal anisotropy from Eq. (21) of 2.7. This value of the longitudinal anisotropy is too small by a factor of 10 to account for the experimentally observed value (which is 30). Thus interactions of longitudinal phonons with electrons in the α and β sheets of the Fermi surface cannot account for the strong anisotropy of the attenuation of longitudinal phonons observed in Sr_2RuO_4,[1] and these interactions must be dominated by other interactions.

Now suppose that the attenuation of longitudinal phonons is dominated by their interaction with electrons in the γ band and neglect the contribution to the attenuation from electrons in the xz and yz bands. The longitudinal anisotropy in this case is given by

$$\frac{\eta_{L100}}{\eta_{L110}} = \frac{\langle\cos^2(k_x a)\rangle_\gamma - p^\gamma\langle\cos(k_x a)\rangle_\gamma}{\langle\{\frac{1}{2}[\cos(k_x a)+\cos(k_y a)]\}^2\rangle_\gamma - p^\gamma\langle\cos(k_x a)\rangle_\gamma}. \tag{22}$$

Here the subscript γ on the angular brackets (as in $\langle\rangle_\gamma$) indicates that the average is over the γ sheet of the Fermi surface only. To begin with, for the purposes of obtaining a qualitative understanding of Eq. (22), neglect $\langle\cos(k_x a)\rangle_\gamma$

since numerical estimates show that it is small. Now note that at the X point of the Fermi surface, $k_x a = \pi$ and $k_y = 0$, so $\cos(k_x a) + \cos(k_y a) = 0$. Because the γ sheet of the Fermi surface passes close to this point, the value of $\cos(k_x a) + \cos(k_y a)$ will be small here and this will contribute to a large value of the longitudinal anisotropy. Furthermore, it should be noted that the X point is a saddle point of the electron energy versus $\mathbf{k}$ surface, so that the Fermi velocity $v_{\mathbf{k}}$ goes to zero there. This means that in carrying out the Fermi-surface average using Eq. (8), points close to the X point will be more heavily weighted, thus further enhancing the magnitude of the longitudinal anisotropy. To obtain an explicit value for the longitudinal anisotropy, we make use of the tight-binding approximation to $\varepsilon_{\mathbf{k}}$ given in Ref. 13, with the parameters given in that article. Thus we use, for the electron energy in the γ band, $\epsilon_{\mathbf{k}} = E_0 + 2t[\cos(k_x a) + \cos(k_y a)] + 4t' \cos(k_x a)\cos(k_y a)$, with parameters $(E_0 - E_F, t, t') = (-0.4, -0.4, -0.12)$. This allows Eq. (22) to be evaluated numerically [including now the relatively small effect of a nonzero $\langle \cos(k_x a) \rangle_\gamma$], giving the result $(\eta_{L100}/\eta_{L110}) = 37$. This is in reasonable agreement with the experimentally determined value of approximately 30 (see Fig. 1), considering the fact that no attempt was made to adjust the Fermi-surface parameters to improve the agreement and that the inclusion of a relatively small contribution from the less anisotropic attenuation due the the xz and yz electrons would also reduce the calculated longitudinal anisotropy. The conclusion is that electrons on the γ sheet of the Fermi surface give the dominant contribution to the ultrasonic attenuation and that the detailed Fermi-surface structure for electrons on the γ sheet is important for understanding the large anisotropy in the attenuation of the longitudinal sound waves.

So far, only the effect of the nearest-neighbor electron-phonon interactions on the ultrasonic attenuation has been discussed. Note that for these interactions, the ultrasonic attenuation of the T100 waves is zero [see Eqs. (15), (18), and (19) for $\phi = 0$]. This is because transverse waves propagating in the 100 direction do not stretch the nearest-neighbor bonds. Such waves do, however, stretch the next-nearest-neighbor bonds, and attenuation of the T100 waves from the next-nearest-neighbor electron-phonon interaction is to be expected. This attenuation associated with T_1 basal-plane phonons interacting with γ-sheet electrons can be found in terms of the quantity

$$F'^{\gamma}_{T1}(\mathbf{k}, \mathbf{q}) = g'^{\gamma} \cos(2\phi) \sin(k_x a) \sin(k_y a). \tag{23}$$

The fact that the attenuation of the T100 phonons is about 1000 times smaller than that of the L100 or T110 phonons is a good indication that, in Sr_2RuO_4 the next-nearest-neighbor electron-phonon interactions are in general less important than the near-neighbor interactions.

The formula

$$\frac{\eta_{T100}}{\eta_{L100}} = \left(\frac{g'^{\gamma}}{g^{\gamma}} \right)^2 \frac{\langle \sin^2(k_x a) \sin^2(k_y a) \rangle_{FS}}{\langle \cos^2(k_x a) \rangle_{FS}} \tag{24}$$

[from Eqs. (14) and (23)], together with the experimentally measured values of the viscosities η_{T100} and η_{L100}, can be used to put an upper limit on the magnitude of g'^{γ}/g^{γ} of 0.041. This is an upper limit because, as will be argued below, a different interaction could be responsible for the T100 attenuation. This upper limit is surprisingly small, given that the ratio of the next-nearest-neighbor to nearest-neighbor hopping matrix elements for the γ band as estimated from the parameters assumed in Ref. 13 is about 0.3. There is, however, no *a priori* reason why the sensitivity of a hopping matrix element to bond stretching should be directly proportional to the magnitude of the matrix element itself.

There is at present no experimental information on the attenuation of T_2 phonons: i.e., by definition those transverse phonons with their propagation vector $\mathbf{q}$ lying in the basal plane and their direction of polarization perpendicular to the basal plane. The attenuation obtained from a consideration of the body-diagonal electron-phonon interaction described above is given in terms of

$$F^{\xi z, \eta z}_{T2}(\mathbf{k}, \mathbf{q}) = g^{\xi z, \eta z} [\cos\phi \sin(\tfrac{1}{2} k_x a) \cos(\tfrac{1}{2} k_y a) + \sin\phi \cos(\tfrac{1}{2} k_x a) \sin(\tfrac{1}{2} k_y a)] \sin(\tfrac{1}{2} k_z c). \tag{25}$$

Some factors of order unity have been absorbed into the definition of $g^{\xi z, \eta z}$. When squared and averaged over the Fermi surface, this formula gives an attenuation independent of the direction of $\mathbf{q}$ in the basal plane.

Similarly, the attenuation of T_1 phonons by the body-diagonal electron-phonon interaction with the xz and yz bands is described by

$$F^{\xi z, \eta z}_{T1}(\mathbf{k}, \mathbf{q}) = \alpha g^{\xi z, \eta z} \cos(2\phi) \cos(\tfrac{1}{2} k_z c) \times \sin(\tfrac{1}{2} k_x a) \sin(\tfrac{1}{2} k_y a). \tag{26}$$

Here, α is a numerical constant of order unity. The interaction of T_1 phonons by the body-diagonal electron-phonon interaction with the γ-sheet electrons is described by an identical formula, except we put $\alpha = 1$ and call the coupling constant g''^{γ}.

IV. ULTRASONIC ATTENUATION IN THE SUPERCONDUCTING STATE

Now that a satisfactory model for the electron-phonon interaction has been established, it is possible to proceed with confidence to an interpretation of the ultrasonic attenuation measurements [1] performed in the superconducting state of Sr_2RuO_4. The basic idea is to use the principles described by Moreno and Coleman[2] to gain information about the location of the gap nodes in Sr_2RuO_4. Evidence for the existence of gap nodes, some of which is presented in Fig. 1 from Ref. 1, has been summarized in the Introduction.

At low temperatures in a superconductor with gap nodes, only Bogoliubov quasiparticles in the neighborhood of the nodes are thermally excited, and hence only these quasiparticles can interact with the phonons to absorb them (and thus

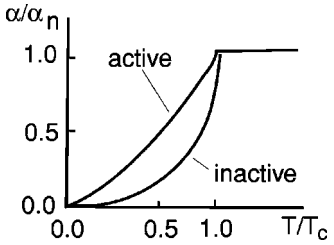

FIG. 3. Qualitative behavior of the ultrasonic attenuation relative to that in the normal state vs temperature relative to T_c. The attenuation of sound for the case where only inactive nodes are present grows more slowly by a factor of T^2 relative to that where active nodes are present, at temperatures well below T_c.

to attenuate a sound wave). The lifetime of a phonon is given by Eq. (7). Everything depends on the behavior of the electron-phonon matrix element $\tilde{F}_j(\mathbf{k},\mathbf{q})$ at the wave vectors $\mathbf{k}$ corresponding to the nodes. If this matrix element is nonzero at the nodes for a particular phonon, then the phonon can interact well with the nodal Bogoliubov quasiparticles, and the nodes are said to be active for that particular phonon. If, on the other hand, the matrix element is zero at the nodes for a particular phonon, then the coupling of the phonon to Bogoliubov quasiparticle precisely at the node is zero and grows as the distance from the node is increased. In this case, the nodes are said to be inactive for the phonon in question. The ultrasonic attenuation at temperatures well below the gap in the case where only inactive nodes are present is proportional to T^2 times the ultrasonic attenuation when active nodes are present,[2] as illustrated in Fig. 3.

Suppose that the only nodes in the superconducting gap are vertical line nodes in the (110) planes. Then it is clear from Eq. (15) that the electron-phonon matrix element for the T110 phonon is zero at the nodes [since $k_x=\pm k_y$ for $\mathbf{k}$ in a (110) plane], and (110) nodes are thus inactive for the T110 phonon. For T100 phonons, the nearest-neighbor electron-phonon matrix element of Eq. (15) is zero for all $\mathbf{k}$ because $\phi=0$. Thus, for the T100 phonon, its activity is determined by the next-nearest-neighbor interaction given by Eq. (23) or Eq. (26), which shows that the T100 phonon is active for nodes in the (110) planes. Similarly, Eq. (14) can be used to show that the electron-phonon matrix element $\tilde{F}$ is nonzero at nodes in (110) planes for both L100 ($\phi=0$) and L110 ($\phi=\pi/4$) phonons, showing that both of these modes are active. Thus, if the only nodes in the gap are those in (110) planes, the attenuation of the T110 sound wave would increase significantly more slowly on increasing the temperature from zero than that of the T100, L100, or L110 sound waves. From Fig. 1 this is clearly not the case, thus ruling out states that have nodes only in (110) planes. In particular this rules out a superconducting spin-singlet state of $k_x^2-k_y^2$ symmetry, as well as a spin-triplet f state with $\mathbf{d}=\hat{\mathbf{z}}(k_x+ik_y)(k_x^2-k_y^2)$.

Next consider the case that the only nodes in the superconducting gap are vertical line nodes in the (100) planes. Arguments similar to those given above show that these (100) nodes are active for L100, L110, and T110 sound waves, but inactive for T100 sound waves. In this case the attenuation of the T100 sound wave should increase markedly more slowly with temperature at low temperatures than that of the other three sound-wave types, and this is not the case. This rules out states that have only (100) line nodes, such as the f-wave state with $\mathbf{d}=\hat{\mathbf{z}}(k_x+ik_y)k_xk_y$.

The arguments of the previous paragraphs have ignored the effects of the α and β sheets of the Fermi surface. Our implementation of our model is inaccurate for the behavior of the electron-phonon matrix element at (110) nodes for the α and β sheets of the Fermi surface because we have not taken into account properly the hybridization of the xz and yz bands, which is important in the [110] directions. A more detailed discussion could be given to remedy this deficiency. This will not be necessary, however, as it will be seen that the more general and powerful symmetry arguments of the following section confirm the conclusions reached above.

It should be noted that the electron-phonon interaction developed in this article gives results that are significantly different from those obtained when the electron-phonon interaction is formulated in terms of an isotropic electron stress tensor (e.g., see Refs. 2, 10, and 11). This can seen, for example, in the top panel of Fig. 2 of Ref. 11, where a model with gap nodes in (110) planes is analyzed, and the L100 mode shows behavior characteristic of interaction with inactive nodes, since its calculated attenuation grows much more slowly as the temperature is increased from zero than the calculated attenuation of the T100 mode. As noted in Ref. 11, the intensity of the coupling of the L100 phonon to the electrons in the isotropic electron–stress-tensor model is proportional to the factor $(\hat{k}_x^2-\frac{1}{2})^2$, which is zero in (110) planes, making the (110) nodes inactive. This inactivity of the (110) nodes for the L100 phonon is an ''accidental'' inactivity; i.e., it is a particularity of the isotropic electron–stress-tensor electron-phonon interaction which would not be present in a more general model and (as demonstrated in the follow section) is not required by symmetry. In fact, as shown above, the (110) nodes are active for L100 phonons for the electron-phonon interaction developed in this article. Thus it seems clear that the isotropic electron–stress-tensor model should not be used in interpretations of ultrasonic attenuation experiments which aim at locating the positions of the gap nodes in an unconventional superconductor.

Finally note that the electron-phonon matrix element for the attenuation of transverse T_2 phonons in Sr_2RuO_4 (i.e., those that have a propagation vector $\mathbf{q}$ in the basal plane and a polarization perpendicular to the basal plane) is given by Eq. (25). The factor $\sin(k_zc/2)$ contained in this expression means that this matrix element is zero for horizonal nodes lying in the plane $k_z=0$ or on the $k_z=2\pi/c$ surface of the Brillouin zone. Thus, horizontal nodes at $k_z=0$ or at $k_z=2\pi/c$ are inactive for T_2 phonons, and the comparison of the attenuation for T_2 phonons with that for other active phonons can be used as a test for such nodes. Unfortunately, it is more difficult to find a definitive test for horizontal nodes that might appear at $k_z=\pi/c$, such as in the proposal of Ref. 30, since there does not appear to be any phonon mode that is inactive for such nodes. This is related to the

fact that such nodes are not required by the symmetry of the order parameter, but are accidental.

So far we have investigated only the effects of the relatively large differences in the temperature dependence of the attenuation that are expected to occur as a result of the differences between active and inactive nodes. Such differences do not appear to occur in the experimental results currently available for Sr_2RuO_4. There is, however, an intriguing smaller difference in the temperature dependence noted by Lupien *et al.*[1] This is that the ratio of the attenuation of the T100 mode in the superconducting state to its normal-state value is somewhat larger at low temperatures than that of the other measured sound wave modes (see Fig. 1). This attenuation is much smaller than that of the other measured sound-wave modes and was accounted for above in terms of a second-neighbor intraplanar electron-phonon interaction. This is not the only possibility, however. It is possible that the interplanar body-diagonal electron-phonon interaction could be the most important for this mode. This interaction has the characteristic feature that the squared matrix element contains the factor $\cos^2(k_z c/2)$. If there are horizontal nodes close to either the $k_z=0$ or $k_z=2\pi/c$ planes where this factor has its maximum, then this would give the T100 sound-wave modes a boost in attenuation at low temperatures relative to the other observed nodes, in agreement with experiment.

In summary, the results of ultrasonic attenuation experiments,[1] when looked at in the light of the above-theoretical considerations, provide evidence against vertical line nodes in either the [100] or [110] plane. Also, the experiments are consistent with horizontal line nodes. Finally, as to the positions of the horizontal line nodes, positions close to either the $k_z=0$ or $k_z=2\pi/c$ planes appear to be favored.

V. CRYSTALLOGRAPHIC SYMMETRY, THE ELECTRON-PHONON INTERACTION, AND ACTIVE NODES

In the last section an explicit model of the electron-phonon interaction was used to deduce the activity of nodes of different types relative to a given sound-wave mode. While there is reason to believe that the model for the electron-phonon interaction is a relatively good one, since it accounts well for a number of unusual features of the sound attenuation in the normal state of Sr_2RuO_4, it is nevertheless of interest to develop an approach that is not dependent on the details of the particular model. Such an approach, which exploits the crystallographic symmetry, is indeed possible and will now be sketched. Such symmetry arguments will be particularly useful in cases where the electronic structure may not be well known or is sufficiently complicated that a detailed model is difficult to develop.

In this section, the Hamiltonian describing the electron-phonon interaction will be taken to be that of Eq. (3), where the matrix element $g^{\nu}_{\mathbf{k}+\mathbf{q}/2,\mathbf{q},j}$ will be assumed to be completely general and subject only to the restrictions imposed by symmetry. For example, from the properties of the Hermiticity of the Hamiltonian, its time-reversal invariance, and its invariance with respect to spatial inversion in a ruthenium-ion position, it follows that $g^{\nu}_{\mathbf{k}+\mathbf{q}/2,\mathbf{q},j}$ is pure imaginary, is an even function of its argument $\mathbf{k}+\mathbf{q}/2$, and is an odd function of its argument $\mathbf{q}$.

Symmetry arguments can be used to show that, for a transverse phonon with wave vector $\mathbf{q}$ along the [110] direction and its polarization j in the basal plane, perpendicular to $\mathbf{q}$, vertical lines nodes in (110) planes are inactive. Suppose that $\mathbf{k}$ has its basal-plane component in the [110] direction. Then under a reflection in a plane normal to the basal plane and containing $\mathbf{q}$, $c_{\nu,\mathbf{k},\sigma}$ must have a definite parity (i.e., either $c_{\nu,\mathbf{k},\sigma}\rightarrow+c_{\nu,\mathbf{k},\sigma}$ or $c_{\nu,\mathbf{k},\sigma}\rightarrow-c_{\nu,\mathbf{k},\sigma}$). Also, $A_{\mathbf{q},j}\rightarrow -A_{\mathbf{q},j}$. From these properties it follows that $g^{\nu}_{\mathbf{k}+\mathbf{q}/2,\mathbf{q},j}=0$ for all $\mathbf{k}$ lying in the same (110) plane that contains $\mathbf{q}$. A related argument shows that for $\mathbf{k}$ lying in the plane perpendicular to $\mathbf{q}$, $g^{\nu}_{\mathbf{k},\mathbf{q},j}=0$. For this latter argument, it is necessary to assume that $|\mathbf{q}|\ll|\mathbf{k}|$, so that $g^{\nu}_{\mathbf{k}+\mathbf{q}/2,\mathbf{q},j}$ can be replaced by $g^{\nu}_{\mathbf{k},\mathbf{q},j}$. Thus, for a T110 sound wave, the vertical line nodes in the (110) planes are inactive. Furthermore, there are no symmetry arguments that show that (110) nodes are inactive for T100, L100, or L110 sound waves, and they must therefore, in general, be active.

In a similar way it can be shown that symmetry requires that (100) vertical nodes be inactive for T100 sound waves, while these nodes are in general active for T110, L100, and L110 sound waves.

Making use of the fact that the basal plane is a plane of reflection symmetry, one can also show that line nodes in the plane $k_z=0$ and in the plane $k_z=2\pi/c$ are inactive for T_2 sound waves having $\mathbf{q}$ in the basal plane and polarized perpendicular to the basal plane.

In the long-wavelength limit $|\mathbf{q}|\ll|\mathbf{k}|$, the symmetry arguments given above can be formulated in a particularly simple form. In this limit, the function $\tilde{F}^{\nu}_{j}(\mathbf{k},\mathbf{q})$ determining the symmetry of the electron-phonon interaction [and which can be obtained from Eqs. (9) and (6)] can be written as

$$\tilde{F}^{\nu}_{j}(\mathbf{k},\mathbf{q})=g^{\nu}\sum_{\alpha,\beta=x,y,z} f^{\nu}_{\alpha\beta}(\mathbf{k})\hat{q}_{\alpha}e_{j,\beta}. \tag{27}$$

(Note that, in the isotropic electron–stress-tensor model, $f_{\alpha\beta}(\mathbf{k})=\hat{k}_{\alpha}\hat{k}_{\beta}-(1/d)\,\delta_{\alpha\beta}$, where d is the dimensionality of the system; this isotropic stress-tensor expression is not used here.) If, for a given $\mathbf{k}$, there is a symmetry operation from the crystallographic point group which leaves $\mathbf{k}$ invariant, but changes the sign of $\hat{q}_{\alpha}e_{j,\beta}$, then the matrix element $f^{\nu}_{\alpha\beta}(\mathbf{k})$ vanishes [one should also use the fact that in symmetry operations, $\mathbf{e}_j$ and $\mathbf{q}$ transform like vectors and $\mathbf{e}_j(-\mathbf{q})=\mathbf{e}_j(\mathbf{q})$]. In particular, one of the consequences is that there are no zeros of $\tilde{F}^{\nu}_{j}(\mathbf{k},\mathbf{q})$ required by symmetry for all longitudinal waves, so the nodes are always active for this polarization. Also, it is clear that a symmetry-imposed line zeros for transverse waves can be present only if $\mathbf{k}$ is in a high-symmetry plane.

Interband transitions of electronic quasiparticles have been ignored in our discussion. Such transitions are expected to play a role only when two bands cross, and since there are relatively few quasiparticles associated with such points,

their effects in general should not be important. However, if a case is encountered where interband transitions play a significant role they will have to be investigated carefully, since the symmetry properties of the electron-phonon matrix element for such transitions are different from those for intraband transitions.

As an application of these ideas to a material with a relatively complicated Fermi surface,[38,39] consider ultrasonic attenuation in UPt_3,[40,41] which is believed to give evidence for the existence of basal-plane line nodes in the superconducting gap. We examine the consequences of the conjecture that the order parameter is characterized by a singlet-state gap $\Delta(k_x,k_y,k_z)$ transforming in accordance with the E_{2g} representation of the point group D_{6h} or by the triplet-state order parameter $d_z(k_x,k_y,k_z)$ which transforms according to E_{2u}. (These are two of the most commonly assumed candidates for the order parameter; e.g., see Ref. 10.) First note that from their symmetry classification, both of these order parameters change sign under reflection in the basal plane. (The space group of UPt_3 is $P6_3/mmc$, which has a σ_z reflection plane.) Hence,

$$\Delta(k_x,k_y,k_z)=-\Delta(k_x,k_y,-k_z),$$

$$d_z(k_x,k_y,k_z)=-d_z(k_x,k_y,-k_z). \tag{28}$$

The constraints of this equation require the order parameters to be zero at $k_z=0$; i.e., there will be a line of nodes wherever a sheet of the Fermi surface cuts the basal plane. [The Fermi surface consists of several sheets,[38,39] with each sheet having its own gap, but all gaps are expected to have the same symmetry and to satisfy Eq. (28).] Note that Eq. (28) also requires the order parameters to be zero at surfaces of the hexagonal Brillouin zone at $k_z=\pm\pi/c$. This is because $(k_x,k_y,+\pi/c)$ and $(k_x,k_y,-\pi/c)$ are equivalent points. There are two toroidal sheets of the Fermi surface that cut the surface $k_z=\pi/c$ of the Brillouin zone[38,39] and hence give line nodes there. The presence of these Brillouin-zone surface line nodes, associated by symmetry with those in the basal plane, does not seem to have been previously noticed.

Because the basal plane of UPt_3 is a plane of reflection symmetry, symmetry arguments similar to those given above show that both basal-plane line nodes and $k_z=\pi/c$ Brillouin-zone-surface line nodes are inactive for T_2 sound waves with $\mathbf{q}\|\mathbf{a}$ and polarization parallel to $\mathbf{c}$, but active for T_1 sound waves with $\mathbf{q}\|\mathbf{a}$ and polarization parallel to $\mathbf{b}$. The temperature dependence of the ultrasonic attenuation data[40,41] shows that the nodes are active for T_1 sound waves and inactive for T_2 sound waves, giving clear evidence of the existence of the basal plane and $k_z=\pi/c$ Brillouin-zone-surface line nodes. These comments extend previous discussions to include Brillouin-zone-surface line nodes and also ensure that the analysis remains valid for the complex Fermi-surface geometry that actually occurs in UPt_3.

VI. CONCLUSIONS

The electron-phonon interaction in Sr_2RuO_4 has a strong anisotropy that is highly unusual. The unusual nature of this interaction can be attributed to certain structural properties of Sr_2RuO_4, these being that the structure is a layered one with a relatively large distance between the RuO_4 layers and that the Ru ions in a layer form a square lattice with the largest electron-phonon interaction being between nearest-neighbor Ru ions. A detailed model electron-phonon interaction based on the idea of a tight-binding Hamiltonian with hopping matrix elements that depend on the ion displacements does a good job of quantitatively accounting for the huge anisotropy observed[1] in ultrasonic attenuation in the normal state of Sr_2RuO_4. The dominant contribution to the attenuation comes from the interaction of phonons with electrons in the γ band. The attenuation of transverse sound waves propagating in the [100] direction and having their polarization in the basal plane is exceptionally small because such waves do not stretch the nearest-neighbor bond lengths and, hence, have no nearest-neighbor electron-phonon interaction. The strong anisotropy for the propagation of longitudinal waves in the basal plane can be related to the fact that the γ sheet of the two-dimensional Fermi surface describes a large circle passing close to the X point of the Brillouin zone. An analysis of the ultrasonic attenuation data[1] in the superconducting state in terms of our model electron-phonon interaction rules out the possibilities that the only nodes in the superconducting gap are vertical lines nodes in (100) planes or vertical line nodes in (110) planes. The experiments performed so far are consistent with the existence of horizontal line nodes such as those proposed in Refs. 29 and 30. With respect to the positions of horizontal line nodes, positions close to the planes $k_z=0$ or $k_z=2\pi/c$ appear to be favored, but a more detailed analysis is need to confirm this.

A general method (based on crystallographic symmetry arguments) of determining the existence of inactive nodes for a given sound wave mode is developed. This method is useful even when it is not possible to develop a detailed microscopic model for the electron-phonon interaction.

As a by-product of our theory, we also propose that the ultrasonic attenuation data in UPt_3 can be interpreted in favor of the existence of horizontal line nodes in the plane $k_z=\pm\pi/c$, as well as in the plane $k_z=0$.

Our results, both for the anisotropy of the ultrasonic attenuation in the normal state and for questions related to the positions of gap nodes in the superconducting state, are different from those obtained when using the traditional method of modeling the electron-phonon interaction in terms of an isotropic electron stress tensor. In particular, the isotropic electron–stress-tensor model makes certain superconducting gap nodes accidentally inactive, when they are in fact active.

Note added in proof. A fundamental justification of our Eq. (9) has been given in terms of a model explicitly including Coulomb interactions between the electrons in Ref. 48. We would like to thank V. Mineev for drawing this article to our attention.

ACKNOWLEDGMENTS

We thank L. Taillefer, C. Lupien, and A. MacFarlane for stimulating discussions, and C. Lupien for providing us with Fig. 1. The hospitality of Efim Kats and the Theory Group of the Institut Laue Langevin, where some of this work was

done, is much appreciated, as is the support of the Canadian Institute for Advanced Research and of the Natural Sciences and Engineering Research Council of Canada.

APPENDIX: SYMMETRY AND UNIVERSALITY OF ULTRASONIC ATTENUATION

One of the remarkable features of unconventional superconductors is that some of their transport coefficients attain ''universal'' (i.e., independent of the disorder concentration) values at sufficiently low temperatures. In particular, universality was first predicted for electrical conductivity of *d*-wave superconductors in Ref. 42 (see also Ref. 43) and for thermal conductivity in Refs. 44 and 45 and observed experimentally in thermal conductivity in Ref. 46. In this appendix, we study the low-temperature behavior of ultrasonic attenuation in unconventional superconductors, using the model formulated in Sec. II.

In the absence of vertex corrections, the ultrasonic attenuation coefficient in the hydrodynamic approximation is given by

$$\frac{\alpha_j(\mathbf{q},T)}{\alpha_j(\mathbf{q},T_c)}=\frac{1}{\tau_n}\int_0^\infty d\epsilon\left(-\frac{\partial f}{\partial\epsilon}\right)\frac{A_j(\mathbf{q},\epsilon)}{\mathrm{Re}\ \tilde{\epsilon}(\epsilon)}, \tag{A1}$$

where $j=L,T_1,T_2$ labels the phonon polarization and

$$A_j(\mathbf{q},\epsilon)=\frac{1}{2\ \mathrm{Im}\ \tilde{\epsilon}(\epsilon)}\langle\tilde{F}_j^2(\mathbf{k},\mathbf{q})\rangle_{FS}^{-1} \times\left\langle \tilde{F}_j^2(\mathbf{k},\mathbf{q})\ \mathrm{Re}\ \frac{|\tilde{\epsilon}(\epsilon)|^2+\tilde{\epsilon}^2(\epsilon)-2|\Delta_\mathbf{k}|^2}{\sqrt{\tilde{\epsilon}^2(\epsilon)-|\Delta_\mathbf{k}|^2}}\right\rangle_{FS}. \tag{A2}$$

The temperature-independent ultrasonic attenuation in the normal state is given by

$$\alpha_j(\mathbf{q},T_c)=\frac{8\omega_{\mathbf{q},j}^2}{\rho v_j^3}N_F\tau_n\langle\tilde{F}_j^2(\mathbf{k},\mathbf{q})\rangle_{FS}. \tag{A3}$$

The expression (A1) is similar to that given in Ref. 3, the only difference being in the angular dependence of the electron-phonon interaction (see also Ref. 6). To reproduce the results obtained with the help of the isotropic electron stress tensor, one should replace $\tilde{F}_j(\mathbf{k},\mathbf{q})\to(\hat{\mathbf{k}}\cdot\hat{\mathbf{q}})[\hat{\mathbf{k}}\cdot\mathbf{e}_j(\mathbf{q})]-(1/d)[\hat{\mathbf{q}}\cdot\mathbf{e}_j(\mathbf{q})]$.

The function $\tilde{\epsilon}(\epsilon)$ describes the self-consistent renormalization of quasiparticle energy due to impurity scattering and satisfies the equation

$$\tilde{\epsilon}=\epsilon+\frac{i}{2\tau_n}\frac{g(\tilde{\epsilon})}{\cos^2\delta_0+g^2(\tilde{\epsilon})\sin^2\delta_0}, \tag{A4}$$

where $g(\epsilon)$ is the retarded Green's function G at coinciding points (see Ref. 18 for a review of the effects of disorder in unconventional superconductors). Assuming electron-hole symmetry,

$$g(\epsilon)=\left\langle\frac{\epsilon}{\sqrt{\epsilon^2-|\Delta_\mathbf{k}|^2}}\right\rangle_{FS}. \tag{A5}$$

In particular, for quasi-2D *d*-wave order parameters $\Delta_\mathbf{k}=\Delta_0\cos 2\varphi$ ($d_{x^2-y^2}$ symmetry) or $\Delta_\mathbf{k}=\Delta_0\sin 2\varphi$ (d_{xy} symmetry) and a cylindrical Fermi surface, $g(\epsilon)=(2/\pi)K(\Delta_0/\epsilon)$, where $K(x)$ is the complete elliptic integral. The function $\tilde{\epsilon}(\epsilon)$ determines, for example, the inverse mean free time of quasiparticles,

$$\frac{1}{\tau(\epsilon)}=2\ \mathrm{Im}\ \tilde{\epsilon}(\epsilon), \tag{A6}$$

and the disorder-averaged quasiparticle density of states (DOS):

$$N(\epsilon)=N_F\ \mathrm{Re}\ g(\tilde{\epsilon}(\epsilon)). \tag{A7}$$

The behavior of the attenuation coefficient strongly depends on the value of the phase shift δ_0. Here we consider two limiting cases of weak impurities (Born limit), when $\delta_0\to 0$, and strong impurities (unitary limit), when $\delta_0\to\pi/2$.

The solution of Eq. (A4) at zero energy is purely imaginary in both cases: $\tilde{\epsilon}(\epsilon=0)=i\Gamma_0$, where

$$\Gamma_0=\Delta_0\exp(-\pi\Delta_0\tau_n) \tag{A8}$$

in the Born limit and

$$\Gamma_0=\Delta_0\sqrt{\frac{\pi}{2\Delta_0\tau_n\ln\Delta_0\tau_n}} \tag{A9}$$

in the unitary limit. The zero-energy scattering rate Γ_0 determines the crossover energy scale separating two qualitatively different types of the behavior of the observable quantities. If the typical energy of excitations (temperature) is greater than Γ_0, then one can neglect the self-consistent energy renormalization and use the quasiparticle Boltzmann equation for calculating the kinetic properties in the superconducting state (for the application of this approach to unconventional superconductors, see, e.g., Ref. 47). In contrast, if the typical energy is smaller than Γ_0, then the self-consistency effects become important, and the quasiparticle Boltzmann equation is not applicable. In the former case, the imaginary part of $\tilde{\epsilon}$ is small compared to $\mathrm{Re}\ \tilde{\epsilon}\to\epsilon$, and we obtain

$$\frac{\alpha_j(\mathbf{q},T)}{\alpha_j(\mathbf{q},T_c)}=\frac{1}{\tau_n}\int_0^\infty d\epsilon\left(-\frac{\partial f}{\partial\epsilon}\right)\frac{A_j(\mathbf{q},\epsilon)}{\epsilon}, \tag{A10}$$

where

$$A_j(\mathbf{q},\epsilon)=2\tau(\epsilon)\frac{\langle\tilde{F}_j^2(\mathbf{k},\mathbf{q})\ \mathrm{Re}\ \sqrt{\epsilon^2-|\Delta_\mathbf{k}||^2}\rangle_{FS}}{\langle\tilde{F}_j^2(\mathbf{k},\mathbf{q})\rangle_{FS}}. \tag{A11}$$

The expression (A10) is equivalent to Eq. (7) for isotropic impurity scattering. It should be noted that the quasiparticle scattering rate (A6) in the Born limit decreases with energy

in the superconducting state, and at some temperature $T^* \simeq (\omega\tau_n)T_c$ the applicability condition of the hydrodynamic approximation is violated. It turns out, however, that in real experimental conditions for Sr_2RuO_4, the crossover temperature T^* is so small that we neglect this complication here.

In the low-temperature regime, we replace $\mathrm{Im}\,\tilde{\epsilon}$ by Γ_0, take the limit $\mathrm{Re}\,\tilde{\epsilon}\to 0$, calculate the integral over energy, and obtain

$$\frac{\alpha_j(\mathbf{q},T)}{\alpha_j(\mathbf{q},T_c)} = \frac{1}{2\tau_n} \frac{\left\langle \tilde{F}_j^2(\mathbf{k},\mathbf{q}) \dfrac{\Gamma_0^2}{(\Gamma_0^2+|\Delta_\mathbf{k}|^2)^{3/2}} \right\rangle_{FS}}{\langle \tilde{F}_j^2(\mathbf{k},\mathbf{q})\rangle_{FS}}. \tag{A12}$$

We see that, at $T<\Gamma_0$, the ultrasonic attenuation does not depend on temperature.

In the Born limit, for typical disorder concentrations in cuprates and ruthenates, Γ_0 turns out to be exponentially small compared to T_c (in particular, in the experimental conditions of Ref. 1, $\Delta_0\tau_n \sim l_{n,ab}/\xi_{0,ab} \sim 10$, so that $\Gamma_0/T_c < 10^{-3}$). For this reason, only the ''high-temperature'' limit is relevant for Born impurities.

For unitary impurities, however, Γ_0 can be as large as $0.1T_c$, which means that, on one hand, there might be no clear power-law behavior of $\alpha(T)$ at $\Gamma_0 < T \ll T_c$ (it was pointed out, e.g., in Ref. 3), and, on the other hand, the low-temperature regime can be observable. The contributions to the ultrasonic attenuation from active and inactive nodes can be easily separated because of their different dependences on the impurity concentration. For active line nodes at a cylindrical Fermi surface,

$$\left\langle \tilde{F}_j^2(\mathbf{k},\mathbf{q}) \frac{\Gamma_0^2}{(\Gamma_0^2+|\Delta_\mathbf{k}|^2)^{3/2}} \right\rangle_{FS} = \frac{F_0^2}{\pi}\frac{1}{\Delta_0}, \tag{A13}$$

where F_0 is the value of $\tilde{F}_j(\mathbf{k},\mathbf{q})$ at the line of nodes. Therefore, as seen from Eqs. (A3) and (A12), the ultrasonic attenuation does not depend on the impurity concentration. In contrast, for inactive line nodes,

$$\left\langle \tilde{F}_j^2(\mathbf{k},\mathbf{q}) \frac{\Gamma_0^2}{(\Gamma_0^2+|\Delta_\mathbf{k}|^2)^{3/2}} \right\rangle_{FS} = \frac{F_0'^2}{\pi}\frac{\Gamma_0^2}{\Delta_0^3}\ln\frac{\Delta_0}{\Gamma_0}, \tag{A14}$$

where F_0' is the value of the transverse derivative of $\tilde{F}_j(\mathbf{k},\mathbf{q})$ at the line of nodes. Therefore, in this case, the ultrasonic attenuation does depend on the impurity concentration. Comparing Eqs. (A13) and (A14), we see that the contribution from inactive nodes is typically much smaller than that from active ones, and one can make a conclusion that if, for a given polarization and propagation, there are active nodes present, the attenuation coefficient is universal at low temperatures. In particular, the attenuation of longitudinal waves should always be universal. On the other hand, for example, the attenuation of the in-plane T_2 waves for the order parameters with horizontal line nodes at $k_z=0$ cannot be universal, because such nodes are inactive. Also, for an *f*-wave order parameter $\mathbf{d}(\mathbf{k}) \propto \hat{\mathbf{z}}(k_x+ik_y)k_xk_y$, the attenuation coefficient of the T110 phonons is universal, whereas that of the T100 phonons is not. For the order parameter $\mathbf{d}(\mathbf{k}) \propto \hat{\mathbf{z}}(k_x+ik_y)(k_x^2-k_y^2)$ the situation is opposite: the T100 attenuation is universal, but T110 is not. It should be noted that the calculations based on the isotropic electron–stress-tensor model give different results.[6]

[1] C. Lupien, W. A. MacFarlane, C. Proust, L. Taillefer, Z. Q. Mao, and Y. Maeno, Phys. Rev. Lett. **86**, 5986 (2001).
[2] J. Moreno and P. Coleman, Phys. Rev. B **53**, R2995 (1996).
[3] P. Hirschfeld, D. Vollhardt, and P. Wölfle, Solid State Commun. **59**, 111 (1986).
[4] K. Scharnberg, D. Walker, H. Monien, L. Tewordt, and R. A. Klemm, Solid State Commun. **60**, 535 (1986).
[5] S. Schmitt-Rink, K. Miyake, and C. M. Varma, Phys. Rev. Lett. **57**, 2575 (1986).
[6] M. J. Graf, S.-L. Yip, and J. A. Sauls, Phys. Rev. B **62**, 14 393 (2000).
[7] T. Tsuneto, Phys. Rev. **121**, 402 (1961).
[8] L. P. Kadanoff and I. I. Falko, Phys. Rev. **136**, A1170 (1964).
[9] E. I. Blount, Phys. Rev. **114**, 418 (1959).
[10] M. J. Graf and A. V. Balatsky, Phys. Rev. B **62**, 9697 (2000).
[11] W. C. Wu and R. Joynt, Phys. Rev. B **64**, 100507 (2001).
[12] D. F. Agterberg, T. M. Rice, and M. Sigrist, Phys. Rev. Lett. **78**, 3374 (1997).
[13] I. I. Mazin and D. J. Singh, Phys. Rev. Lett. **79**, 733 (1997).
[14] I. Vekhter, E. J. Nicol, and J. P. Carbotte, Phys. Rev. B **59**, 7123 (1999).
[15] Y. Maeno, H. Hashimoto, K. Yoshida, S. NishiZaki, T. Fujita, J. G. Bednorz, and F. Lichtenberg, Nature (London) **372**, 532 (1994).
[16] T. M. Rice and M. Sigrist, J. Phys.: Condens. Matter **7**, L643 (1995).
[17] Y. Maeno, T. M. Rice, and M. Sigrist, Phys. Today **54** (1), 42 (2001).
[18] V. P. Mineev and K. V. Samokhin, *Introduction to Unconventional Superconductivity* (Gordon and Breach, Amsterdam, 1999).
[19] A. P. Mackenzie, S. R. Julian, A. J. Diver, G. G. Lonzarich, Y. Maeno, S. NishiZaki, and T. Fujita, Phys. Rev. Lett. **76**, 3786 (1996).
[20] S. NishiZaki, Y. Maeno, and Z. Mao, J. Low Temp. Phys. **117**, 1581 (1999).
[21] S. NishiZaki, Y. Maeno, and Z. Mao, J. Phys. Soc. Jpn. **69**, 572 (2000).
[22] K. Ishida, H. Mukuda, Y. Kitaoka, Z. Q. Mao, Y. Mori, and Y. Maeno, Phys. Rev. Lett. **84**, 5387 (2000).
[23] I. Bonalde, B. D. Yanoff, M. B. Salamon, D. J. Van Harlingen, and E. M. E. Chia, Phys. Rev. Lett. **85**, 4775 (2000).
[24] M. A. Tanatar, S. Nagai, Z. Q. Mao, Y. Maeno, and T. Ishiguro, Phys. Rev. B **63**, 064505 (2001).
[25] K. Izawa, H. Takahashi, H. Yamaguchi, Y. Matsuda, M. Suzuki, T. Sasaki, T. Fukase, Y. Yoshida, R. Settai, and Y. Onuki, Phys. Rev. Lett. **87**, 057002 (2001).

[26] K. Miyake and O. Narikiyo, Phys. Rev. Lett. **83**, 1423 (1999).
[27] T. Dahm, H. Won, and K. Maki, cond-mat/0006301 (unpublished).
[28] T. Kuwabara and M. Ogata, Phys. Rev. Lett. **85**, 4586 (2000).
[29] Y. Hasegawa, K. Machida, and M. Ozaki, J. Phys. Soc. Jpn. **69**, 336 (2000).
[30] M. Zhitomirsky and T. M. Rice, Phys. Rev. Lett. **87**, 057001 (2001).
[31] H. Won and K. Maki, cond-mat/0006151 (unpublished).
[32] K. Maki and G. Yang, Fiz. A **8**, 345 (1999).
[33] T. Oguchi, Phys. Rev. B **51**, 1385 (1995).
[34] D. J. Singh, Phys. Rev. B **52**, 1358 (1995).
[35] A. I. Akhiezer, M. I. Kaganov, and G. Ia. Liubarskii, JETP Lett. **5**, 685 (1957); see also A. A. Abrikosov, *Introduction to the Theory of Normal Metals* (Academic Press, New York, 1972).
[36] L. D. Landau and E. M. Lifshitz, *Theory of Elasticity* (Pergamon Press, Oxford, 1975).
[37] C. Bergemann, S. R. Julian, A. P. Mackenzie, S. Nishizaki, and Y. Maeno, Phys. Rev. Lett. **84**, 2662 (2000).
[38] L. Taillefer, R. Newbury, G. G. Lonzarich, Z. Fisk, and J. L. Smith, J. Magn. Magn. Mater. **63&64**, 372 (1987).
[39] T. Oguchi, A. J. Freeman, and G. W. Crabtree, J. Magn. Magn. Mater. **63&64**, 645 (1987).
[40] B. S. Shivaram, Y. H. Jeong, T. F. Rosenbaum, and D. G. Hinks, Phys. Rev. Lett. **56**, 1078 (1986).
[41] B. Ellman, L. Taillefer, and M. Poirer, Phys. Rev. B **54**, 9043 (1996).
[42] P. A. Lee, Phys. Rev. Lett. **71**, 1887 (1993).
[43] Y. Sun and K. Maki, Phys. Rev. B **51**, 6059 (1995).
[44] M. R. Norman and P. J. Hirschfeld, Phys. Rev. B **53**, 5706 (1996).
[45] M. J. Graf, S.-K. Yip, J. A. Sauls, and D. Rainer, Phys. Rev. B **53**, 15 147 (1996).
[46] L. Taillefer, B. Lussier, and R. Gagnon, Phys. Rev. Lett. **79**, 483 (1997).
[47] B. Arfi and C. J. Pethick, Phys. Rev. B **38**, 2312 (1988).
[48] A. F. Andreev and Ya. B. Bazalyi, Zh. Eksp. Teor. Fiz. **98**, 1480 (1990) [Sov. Phys. JETP **71**, 827 (1990).